Fully localised nonlinear energy growth optimals in pipe flow

Chris C.T. Pringle,[1] Ashley P. Willis,[2] and Rich R. Kerswell[3]

[1)] *Applied Mathematics Research Centre, Coventry University, Coventry, UK*

[2)] *School of Mathematics and Statistics, University of Sheffield, Sheffield, S3 7RH UK*

[3)] *Department of Mathematics, University of Bristol, Bristol, BS8 1TW, UK*

A new, fully-localised, energy growth optimal is found over large times and in long pipe domains at a given mass flow rate. This optimal emerges at a threshold disturbance energy below which a nonlinear version of the known (streamwise-independent) linear optimal (Schmid & Henningson 1994) is selected, and appears to remain the optimal up until the critical energy at which transition is triggered. The form of this optimal is similar to that found in short pipes (Pringle et al. 2012) albeit now with full localisation in the streamwise direction. This fully-localised optimal perturbation represents the best approximation yet of the *minimal seed* (the smallest perturbation capable of triggering a turbulent episode) for 'real' (laboratory) pipe flows.

arXiv:1408.1414v1 [physics.flu-dyn] 6 Aug 2014

I. INTRODUCTION

In wall-bounded shear flows such as pipe flow, transition to turbulence remains a problem of great theoretical and practical importance. The transition is typically abrupt, occurs at flow rates for which the underlying base flow is stable, and is triggered by disturbance amplitudes much smaller that the ensuing turbulent state. Whether turbulence is triggered or not is also very dependent on the form of the disturbance[1,2] and efforts to identify the best 'shape' have revolved around examining the non-normality of the linearised Navier-Stokes operator around the base state.[3–13] This has identified a number of processes by which a disturbance can grow in energy despite the flow being linearly stable before it has to ultimately decay.[14]

Recently, the approach of finding optimal perturbations that maximise growth over a finite time has been extended to retain the nonlinearity of the Navier-Stokes equations.[15–17] Computationally, this is a very intensive procedure and so far only small computational domains[15,17–19] or short integration times[16,20,21] have been used to demonstrate feasibility of the approach. Nonetheless, it serves as a basis for a proposed procedure for finding the disturbance of the smallest energy – the *minimal seed* – which can trigger transition.[18,22] From a dynamical systems perspective, this minimal seed is the closest point of approach (in the energy norm) of the basin boundary of turbulence (or 'edge' if the turbulent state is only transient) to the basic state and it is clearly of fundamental interest in the problem of transition.

A two stage process has been proposed[18] in which the maximum energy growth across a given time horizon is sought over all disturbances of a given initial energy (the 'nonlinear transient growth problem'), and then the initial energy is increased until a rapid increase in the energy growth is identified. For very large target times this growth increase tends to a discontinuous jump, and the first optimal initial condition (as the initial energy increases) to achieve heightened growth, and thereby be outside the laminar state's basin of attraction, is then an approximation of the minimal seed (see the review[22]). For more moderate optimisation times the jump in energy growth is smoothed, and there is a window in initial energy where a new nonlinear optimal is more efficient than the linear problem's optimal, but where transition cannot be triggered. Provided the time is still larger than the transition time, the amplitude of the minimal seed is also the maximum amplitude of initial perturbation for which convergence is possible. If much shorter times are chosen, it is possible to converge at energies well above this critical amplitude.[21] Intriguingly, provided a long enough time is used, these calculations suggest that the minimal seed should be a fully localised disturbance and therefore of immediate interest to experimentalists.

The purpose of this letter is to carry out this procedure over a long pipe domain to demonstrate that the minimal seed is indeed fully localised when the computational domain is sufficiently long and to obtain the best estimate yet of what the actual minimal seed is for long (real) pipes. The presented work focuses on maximising energy growth (the ratio of energy at time T to initial energy, $G := E(T)/E(0)$) for an intermediate choice of time. In the 25 diameters ($25D$) long pipe being considered, the computational demands of this are already heavy. Nonetheless, the results are shown to be close predictors of the true minimal seed. The paper is split into five further sections: II formulates the problem; III presents and describes the new fully localised nonlinear optimal; IV explores this localisation and shows that the results from much shorter pipes (e.g. $5D$) are closely related; V examines the importance of the choice of optimising time and demonstrates that the observed optimal is largely insensitive to the choice of T, unless exceptionally small values are taken; VI contains a discussion of the results.

II. FORMULATION

We consider the problem of a Newtonian fluid in a straight pipe of circular cross-section. A constant mass-flux is imposed along the pipe, forcing the fluid to flow through it at a constant rate. Nondimensionalising by the pipe radius ($D/2$) and the mean axial velocity (U), the governing equations of motion are

$$\partial_t \mathbf{u} + \mathscr{U}\partial_z \mathbf{u} + u\mathscr{U}'\hat{\mathbf{z}} + \mathbf{u}.\nabla\mathbf{u} = -\nabla p + Re^{-1}\nabla^2\mathbf{u} \tag{1}$$

where $\mathscr{U}\hat{\mathbf{z}} = 2(1-s^2)\hat{\mathbf{z}}$ is the underlying laminar flow to which $\mathbf{u} = (u, v, w)$ is the not-necessarily-small perturbation in cylindrical coordinates (s, ϕ, z). $Re := UD/\nu$ is the Reynolds number. Periodic boundary conditions are imposed across the ends of the pipe (i.e. in z) and no slip conditions on the pipe wall.

We wish to identify the perturbation with initial energy $E_0 := E(0)$ that will undergo the most growth over a given period of time (T), and to this end we employ the usual variational approach[22]. The functional

$$\mathscr{L} := \langle \tfrac{1}{2}\mathbf{u}(\mathbf{x},T)^2\rangle - \lambda\left[\langle \tfrac{1}{2}\mathbf{u}(\mathbf{x},0)^2\rangle - E_0\right] - \int_0^T \langle \boldsymbol{\nu}\cdot\left[\partial_t\mathbf{u} + \mathscr{U}\partial_z\mathbf{u} + u\mathscr{U}'\hat{\mathbf{z}} + \mathbf{u}.\nabla\mathbf{u} + \nabla p - Re^{-1}\nabla^2\mathbf{u}\right]\rangle \mathrm{d}t$$

$$- \int_0^T \langle \Pi\nabla\cdot\mathbf{u}\rangle \mathrm{d}t - \int_0^T \Gamma\langle \mathbf{u}\cdot\hat{\mathbf{z}}\rangle \mathrm{d}t, \tag{2}$$

is maximised numerically in the manner laid out in ref[18]. Throughout this paper we will consider two quantities

$$e(z,t) := \frac{1}{2}\int_0^{2\pi}\int_0^1 \mathbf{u}^2\, s\, ds\, d\phi \qquad \text{and} \qquad E(t) := \frac{1}{2}\int_0^{2\pi/\alpha}\int_0^{2\pi}\int_0^1 \mathbf{u}^2\, s\, ds\, d\phi\, dz = \int_0^{2\pi/\alpha} e(z,t)\, dz. \tag{3}$$

$E(t)$ is the total energy of the perturbation while $e(z,t)$ is the energy per unit length of the perturbation at a given axial position along the pipe at a given time. We also consider the roll and streak energies

$$E_{uv}(t) := \frac{1}{2}\int_0^{2\pi/\alpha}\int_0^{2\pi}\int_0^1 (u,v,0)^2\, s\, ds\, d\phi\, dz \qquad \text{and} \qquad E_w(t) := \frac{1}{2}\int_0^{2\pi/\alpha}\int_0^{2\pi}\int_0^1 (0,0,w)^2\, s\, ds\, d\phi\, dz, \tag{4}$$

with the equivalent versions $e_{uv}(z,t)$ and $e_w(z,t)$ defined in the expected way.

All calculations are performed with 64 finite difference points in s (concentrated near the boundary) and azimuthal Fourier modes running from -23 to 23. For a pipe of length $L = 25D$, we use axial Fourier modes between -128 and 128, while for other lengths of pipe this is adjusted to keep the resolution unaltered. Throughout we use $Re = 2400$ and, except where indicated otherwise, we take the optimisation time to be $T = T_{lin} = 29.35\, D/U$ – the time that maximises the linear optimal growth at this Reynolds number.

III. LOCALISED NONLINEAR OPTIMAL

In order to find the localised nonlinear optimal, we performed the transient growth calculation outlined in section II in a $8\pi \simeq 25$ diameter long pipe. As with shorter domains, for initial energies below a certain threshold (here $E = 1.12\times10^{-4}$), a streamwise independent minor variation of the linear optimal (Quasi-Linear Optimal Perturbation, abbreviated to QLOP) is found. At energies larger than this threshold, a new three dimensional optimal (NonLinear Optimal Perturbation, or NLOP) emerges (Fig. 1, left). The growth produced by the new NLOP quickly dwarfs the energy growth of the corresponding QLOP as the initial energy is increased further, until convergence ceases to be possible and we begin to find turbulent seeds — perturbations that lead to a turbulent end state by $t = T$. To determine the precise point at which convergence fails is beyond the resources available, but it is bounded as follows $1.7\times10^{-4} < E_{fail} < 1.8\times10^{-4}$.

For the nonlinear optimal corresponding to $E_0 = 1.6\times10^4$, we plot cross-sections of the perturbation during its development (Fig. 1, right). The sequence shown is very similar to that observed in shorter pipes.[15,18] Like the previously known optimals, the initial disturbance is strongly localised in the cross-sectional plane and unpacks through a complicated procedure[18] to produce two larger rolls straddling three streaks. Unlike those previously reported, however, the optimal found here is also strongly localised in the streamwise direction with 99% of the energy contained within a $7D$ section of the pipe – shown in Fig. 2. The rolls shown as isosurfaces weave their way along one side of the pipe, threading through the streak contours shown at discrete cross-sections along the pipe. These structures are tightly layered and inclined back into the oncoming flow. This mirrors the structure of the

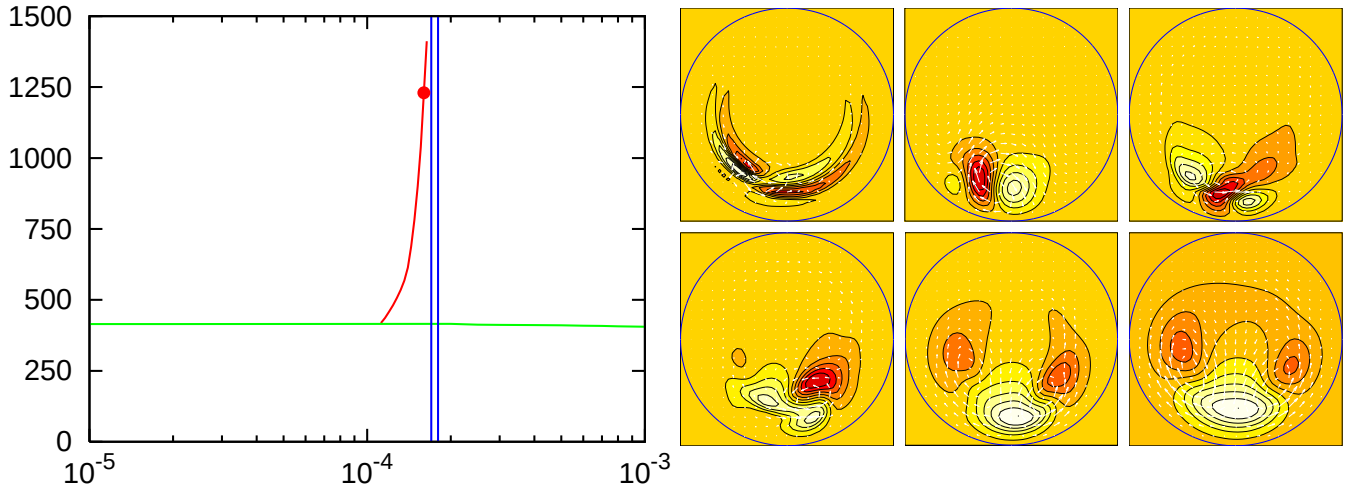

FIG. 1. **Left**: Growth := $E(T_{lin})/E(0)$ as a function of initial energy $E(0)$ for $T = T_{lin}$. The green (almost flat) line is the result of a streamwise-independent, nonlinear calculation. The optimal (QLOP) observed is very similar to the linear optimal. The red (steeply climbing) line shows the new $3D$ optimal NLOP, while the vertical blue lines represent the interval within which turbulent seeds begin to appear. The solid dot indicates the nonlinear optimal at $E_0 = 1.6 \times 10^{-4}$, used as the exemplar localised optimal throughout. **Right**: The evolution of the NLOP in a $25D$ long pipe with $E_0 = 1.6 \times 10^{-4}$. The slices are taken at z corresponding to the maximum value of $e(z,t)$ at times $t = 0$, 1, 2.5, 10, 20 and T_{opt} (all in D/U) (left to right, top to bottom). Streak contour levels are varied between slices to show the structure of the growing disturbance.

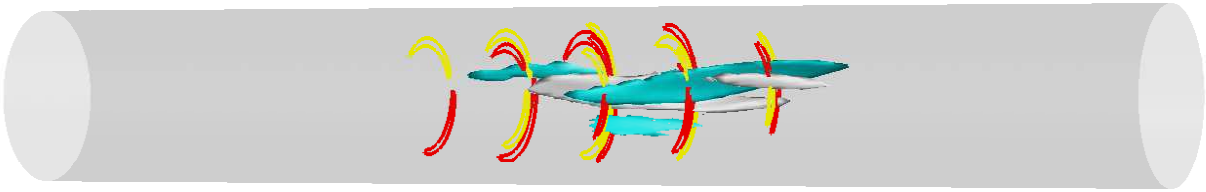

FIG. 2. A $7D$ section of the NLOP from a $25D$ pipe for $E_0 = 1.6 \times 10^{-4}$. The white (cyan) surface is an isosurface of where the vorticity is 30% (−30%) of the maximum vorticity in the pipe. The yellow (red) lines are contours on cross-sectional surfaces of positive (negative) streamwise velocity.

optimal in shorter pipes[18] where the initial growth is driven by the Orr-mechanism in which the layers are tilted up into the underlying shear.

Localisation is present throughout the energy window in which convergence to a nonlinear optimal is possible (Fig. 3). As the initial energy is varied, the streak structure remains essentially unchanged. The roll structure separates slightly in the axial direction as the initial energy is increased leading to two slightly distinct peaks for higher energies.

IV. EFFECT OF L

In order to capture a localised optimal, we must make sure that not only is the optimal initially localised, but that it remains localised throughout its evolution. The perturbation is expected to swell as it grows in energy, and the pipe must be long enough that as it expands it does not begin to interact with itself through the periodic boundary conditions. The degree of self-interaction was tested by repeating the nonlinear transient growth calculation for pipes of length $L = 2\pi D$, $4\pi D$ and $16\pi D \simeq 50D$ at $E_0 = 1.6 \times 10^{-4}$. In Fig. 4, we plot the energy evolution of these optimals along with that of the benchmark $8\pi D \simeq 25D$ optimal. In all four cases the initial evolution is indistinguishable, but as the optimals begin to unfurl along the pipe the evolutions begin to diverge. Unsurprisingly this self-interaction has the greatest effect upon the optimal in the shortest periodic domain. For the $4\pi D$ optimal it is only the very final part of the evolution which is affected, while the $25D$ and $50D$ optimals are indistinguishable. The inset of Fig. 4 shows the initial axial distribution of the energy within these optimals. The central portion of each of these optimals

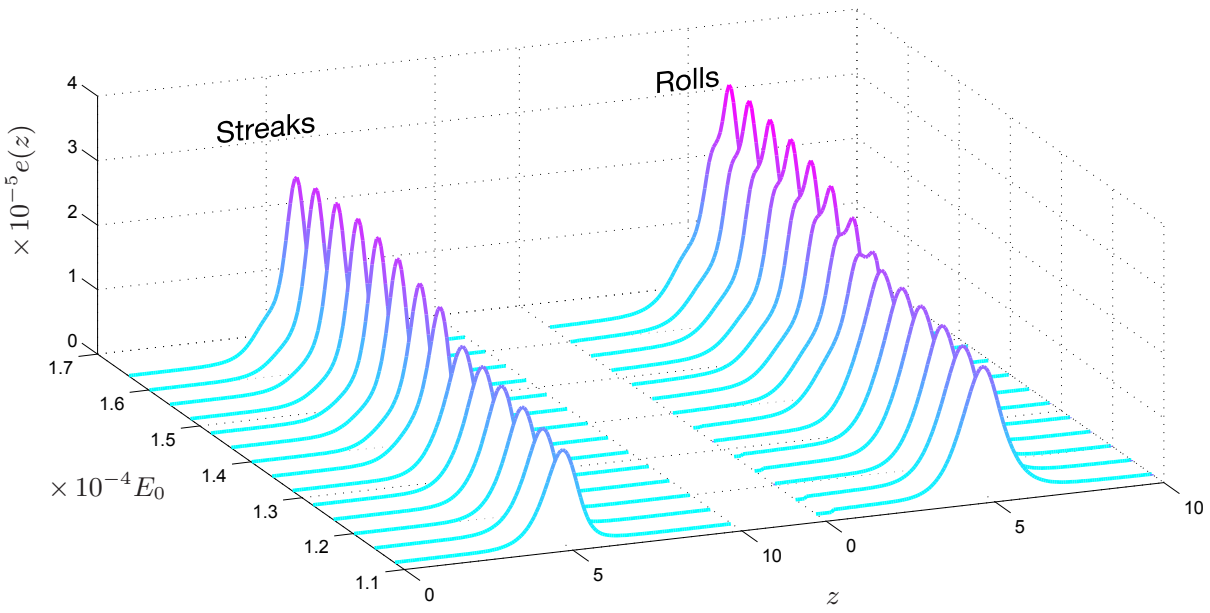

FIG. 3. The axial distribution of the initial energy in the streaks ($e_w(z,0)$) and the rolls ($e_{uv}(z,0)$) of NLOP in a $25D$ pipe, and how it changes as a function of E_0 . z is in units of D so only a $10D$ section of the pipe is represented. The QLOP on this plot would be represented as a flat line of amplitude E_0/L.

align very closely with the distributions only diverging as each optimal reaches the ends of its periodic domain.

Taken altogether, these results suggest that calculations performed in much smaller domains are not only able to capture the same mechanisms and qualitative results as those observed in domains large enough to capture localised dynamics, but that the optimals found are in fact precisely the same. The only apparent difference is that for longer domains there is more space for the energy levels to drop off. This energy drop off is passive and does not directly influence the form of the perturbation.

V. EFFECT OF T

The nonlinear transient growth calculation depends upon the target optimisation time. It has previously been reported that it is possible to converge at high initial amplitudes for which turbulence can be triggered, but this is only if short times are considered.[18,21] The amount of growth also (trivially) varies with this. What is not clear, however, is whether the *form* of the optimal found in the nonlinear calculation also depends upon the choice of target time.

To this end, we performed the nonlinear transient growth calculation for a range of target times. The evolutions of the optimals found through this are shown in Fig. 5. Two separate forms of evolution are observed. For values of $T \gtrsim 16D/U$ the optimals all evolved in similar manners, reaching a peak energy level at $T \simeq 20D/U$ before decaying away. Smaller values of T give an optimal which undergoes an accelerated evolution. The eventual maximum energy levels obtained (were the perturbation allowed to evolve indefinitely) are lower than before, and the transition between these two types of evolution is abrupt – the optimals for $T = 15.5D/U$ and $T = 16D/U$ are indicated by dashed lines in Fig. 5.

Unless short times are taken, the optimal observed is relatively insensitive to the value of T chosen. Previous work[18,22] conjectured, and provided evidence that, if large optimisation times are used then the nonlinear transient growth algorithm can be used to identify both the minimum amplitude of disturbance required to trigger turbulence, and the minimum seed that this equates to. Due to the computationally demanding nature of the computation even in short domains, in this work we have considered intermediate optimisation times. Nonetheless, it appears clear that this is sufficient to observe the *form* of the minimal seed.

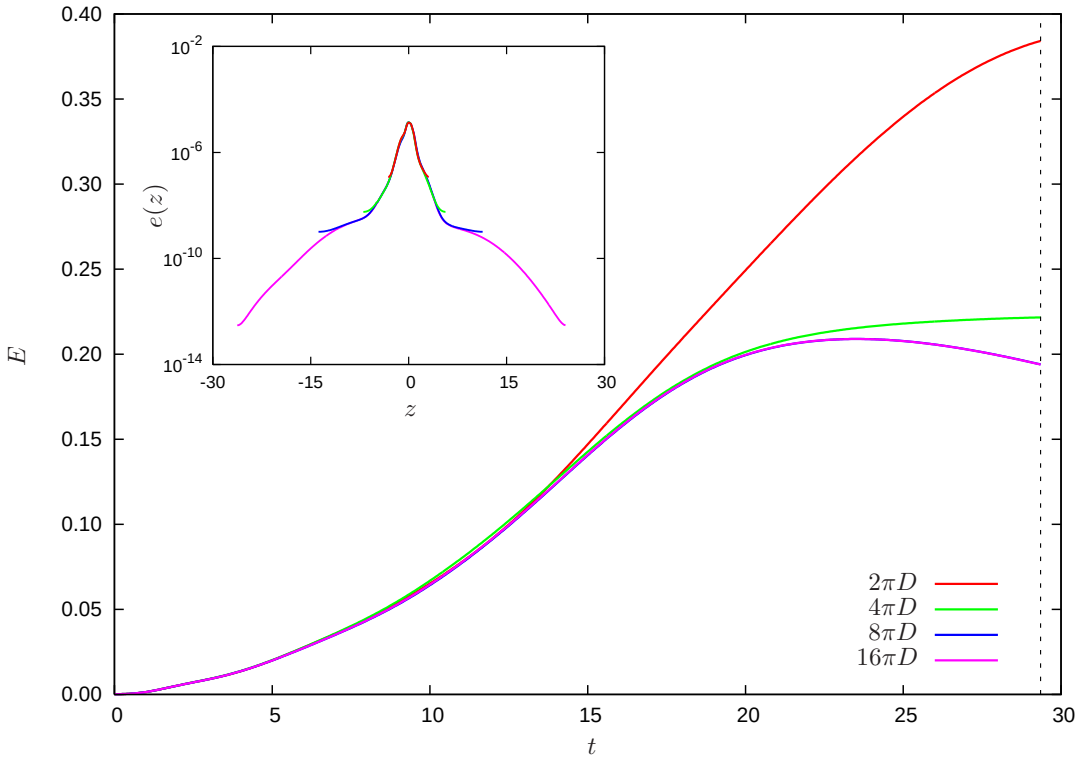

FIG. 4. **Outer:** Evolutions of the NLOPs found in different length pipes at $E_0 = 1.6 \times 10^{-4}$. All four optimals initially have indistinguishable evolutions, before they begin to separate. For the two longest domains they remain inseparable throughout the evolution period. **Inner:** The axial distribution of the initial energy of the same NLOPs. The central structure of the differing optimals closely match, diverging only as the ends of the periodic domain are reached.

VI. DISCUSSION

We have found the first energy growth optimal, which despite the underlying equations supporting strictly periodic domain-filling flows, is fully localised. Reassuringly, this optimal fits well with previous results. The central structure of the optimal is strikingly similar to the optimal found in much shorter domains, and appears to be essentially the same optimal but with an extended region of exponential decay. From this it seems clear the energy growth mechanisms in the localised optimal are essentially the same as for the optimal found in short pipes[18], though now the optimal also expands along the domain as it grows in amplitude. Less clear is what sets the rate of energy drop off in z – a strong scaling appears to be present, but it is not the result of a simple energy balance.

The importance of T has also been illuminated. In order to estimate the minimum amplitude of the edge (E_c) and the minimal seed to high accuracy, large optimisation target times are required. Despite this, the form of the minimal seed is accurately revealed by more intermediate choices. Further, with this choice of T, we were able to find reasonable energy bounds, $1.7 \times 10^{-4} < E_c < 1.8 \times 10^{-4}$. The upper bound is firm as it comes from finding turbulent seeds at this energy.The lower bound is less definite from this calculation alone but is confirmed by performing larger T calculations, for which $E_c = E_{fail}$ - see[18,22]. This estimate for E_c is consistent with the $5D$ result found much more precisely[18] as the slightly lower (since the perturbation can self-interact) value of $E_c = 1.5 \times 10^{-4}$.

It is only when we consider much lower choices of T or very short L that any substantial differences appear. In the case of reducing T, there is an abrupt change where a new optimal emerges which prioritises fast unsustainable growth. A similar change takes place for very short choices of L, where the optimal switches to one exhibiting the shift-and-reflect symmetry

$$\mathcal{S} : (u, v, w)(s, \phi, z) \to (u, -v, w)(s, -\phi, z + L/2); \tag{5}$$

see Fig. 6 which shows that the switchover between the optimals is not a bifurcation as the symmetry-breaking

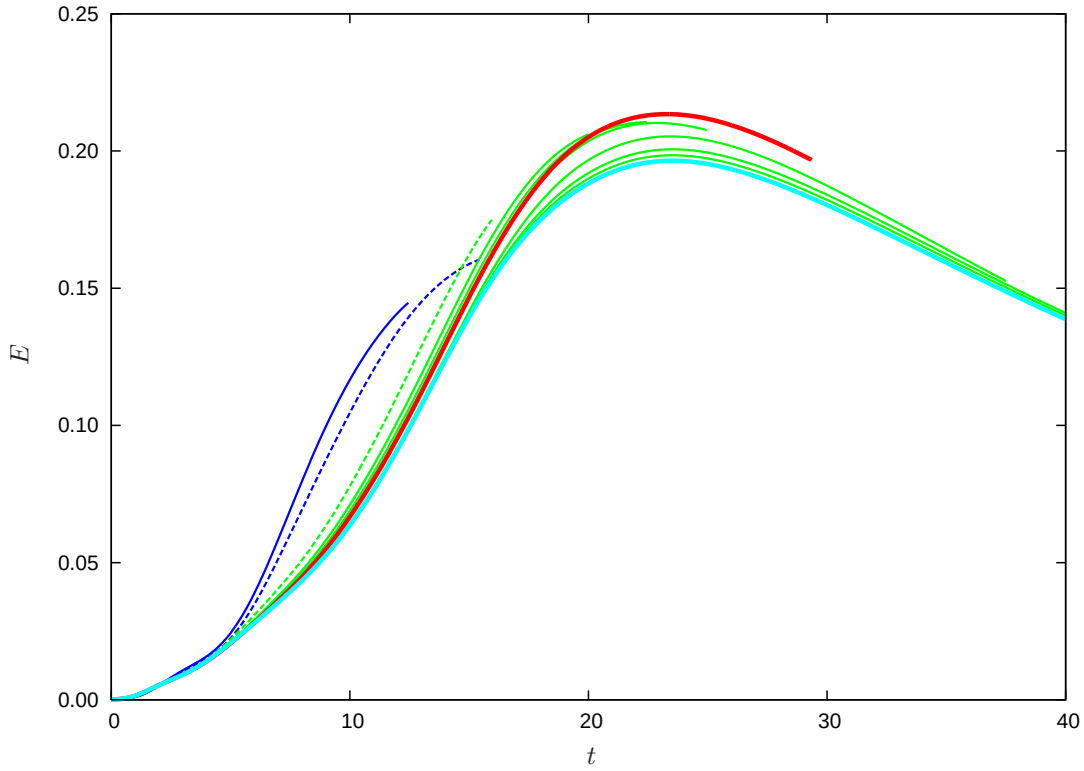

FIG. 5. Evolution of optimals with differing T. The two blue (dark thin)lines have very short optimsation times ($T = 12.5\,D/U$ and $15.5\,D/U$). These two optimals evolve in a notably different manner to all the other optimals ($T \geq 16\,D/U$) being considered. The optimal corresponding to $T = T_{lin}$ is shown in (thick) red, while the largest optimisation time considered ($T = 100D/U$) is shown in cyan (only the first $40\,D/U$ is plotted). The two dashed lines correspond to $T = 15.5\,D/U$ (blue/dark) and $T = 16\,D/U$ (green/light) which bracket the abrupt change in evolution of their respective optimals.

measure

$$dS := \sqrt{\frac{\text{Energy of } (u - \mathcal{S}u)}{\text{Energy of } u}} \tag{6}$$

does not vanish there. This symmetry is unsupportable by a localised disturbance indicating that this is again a fundamentally different perturbation. Outside of these two extreme cases, we have shown that using more computationally viable parameter regimes than those previously stipulated[18] still allows us to ascertain insight into the minimal seed and the corresponding critical minimum amplitude of turbulence. One immediate observation is that the minimal seed has 99% of its energy concentrated in just $7\,D$ of the pipe length at $Re = 2400$. This resonates with the observation in experimental work[23,24] that once disturbances generated by jets become more that $\approx 6\,D$ long, the ensuing dynamics is largely independent of the disturbance length. Recently discovered, localised relative periodic orbits in pipe flow also share this lengthscale of 5-10 D as do turbulent puffs: see figure 2 of ref[25] and figure 4 of ref[26].

In terms of future work, the way is now clear to map out the threshold energy E_c for transition as a function of Re just as has been recently done in small-box plane Couette flow[27] (the imposed streamwise periodicity in[27] is equivalent to $L = 2\pi D$ here). Our results indicate that using small-to-intermediate periodic domains (at least in the streamwise direction) can still yield useful results.

Experimentally, of course, only a small subset Σ of all possible disturbances considered theoretically can actually be generated. To move the theory closer to this reality just requires that the optimisation be performed over Σ which means simply projecting the variational derivative of the energy growth with respect to the initial perturbation down onto Σ. The greater theoretical challenge is actually to accurately model the disturbances routinely generated in the laboratory by injecting or removing fluid through small holes.[23,24] Adding an artificial body force temporarily to the Navier-Stokes equations, however, seems to work well[28].

Another direction to take this work is into control. Here the aim could be to increase E_c by manipulating some

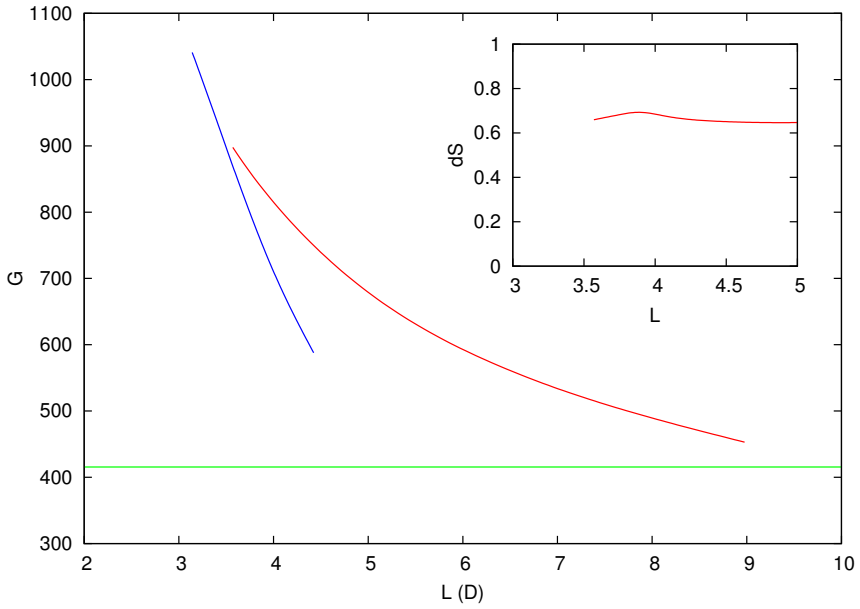

FIG. 6. Growth against length of pipe L (in D) for the streamwise independent optimal, QLOP (green), the nonlinear optimal, NLOP (red) and the nonlinear optimal with shift-and-reflect symmetry enforced with in the domain (blue). The switch in optimal type can clearly be seen at $L \simeq 3.5\,D$ with the shift-and-reflect optimal being the global optimal for shorter domains than this. The inset demonstrates that the switchover is not a bifurcation but merely a crossing over of distinct maximums as the energy in the symmetry-breaking part of the large L optimal does not vanish at the switchover length. All results are for fixed $E_0 = 0.8 \times 10^{-4}$.

aspect of the flow. A first promising step along these lines has already been made in plane Couette flow by oscillating the boundaries in their plane and perpendicular to the shearing direction.[29]

ACKNOWLEDGMENTS

The calculations in this paper were carried out at the Advanced Computing Research Centre, University of Bristol.

[1] A. G. Darbyshire and T. Mullin, "Transition to turbulence in constant-mass-flux pipe-flow," J. Fluid Mech. **289**, 83–114 (1995).
[2] H. Faisst and B. Eckhardt, "Sensitive dependence on initial conditions in transition to turbulence in pipe flow," J. Fluid Mech. **504**, 343–352 (2004).
[3] B. F. Farrell, "Optimal excitation of perturbations in viscous shear flow," Phys. Fluids **31**, 2093–2101 (1988).
[4] B. F. Farrell, "Optimal excitation of baroclinic waves," J. Atmos. Sci. **46**, 1193–1206 (1989).
[5] L. H. Gustavsson, "Energy growth of 3-dimensional disturbances in plane poiseuille flow," J. Fluid Mech. **224**, 241–260 (1991).
[6] K. M. Butler and B. F. Farrell, "3-dimensional optimal perturbations in viscous shear-flow," Phys. Fluids **4**, 1637–1650 (1992).
[7] P. Schmid and D. Henningson, "A new mechanism for rapid transition involving a pair of oblique waves," Phys. Fluids **4**, 1986–1989 (1992).
[8] L. N. Trefethen, A. E. Trefethen, S. C. Reddy, and T. A. Driscoll, "Hydrodynamic stability without eigenvalues," Science **261**, 578–584 (1993).
[9] L. Bergström, "Optimal-growth of small disturbances in pipe Poiseuille flow," Phys. Fluids **5**, 2710–2720 (1993).
[10] S. C. Reddy and D. S. Henningson, "Energy growth in viscous flows," J. Fluid Mech. **365**, 209–238 (1993).
[11] P. J. Schmid and D. S. Henningson, "Optimal energy density growth in Hagen-Poiseuille flow," J. Fluid Mech. **277**, 192–225 (1994).
[12] O. Y. Zikanov, "on the instability of pipe Poiseuille flow," Phys. Fluids **8**, 2923–2932 (1996).
[13] S. C. Reddy, P. J. Schmid, J. S. Baggett, and D. S. Henningson, "On stability of streamwise streaks and transition thresholds in plane channel flows," J. Fluid Mech. **365**, 269–303 (1998).
[14] P. J. Schmid, "Nonmodal stability theory," Annu. Rev. Fl. Mech. **39**, 129–162 (2007).
[15] C. C. T. Pringle and R. R. Kerswell, "Using nonlinear transient growth to construct the minimal seed for shear flow turbulence," Phys. Rev. Lett. **105**, 154502 (2010).
[16] S. Cherubini, P. de Palma, J.-C. Robinet, and A. Bottaro, "Rapid path to transition via nonlinear localised optimal perturbations in a boundary layer flow," Phys. Rev. E **82**, 066302 (2010).
[17] A. Monokrousos, A. Bottaro, L. Brandt, A. Di Vita, and D. S. Henningson, "Nonequilibrium thermodynamics and the optimal path to turbulence in shear flows," Phys. Rev. E **106**, 134502 (2011).
[18] C. C. T. Pringle, A. P. Willis, and R. R. Kerswell, "Minimal seeds for shear flow turbulence: using nonlinear transient growth to touch the edge of chaos," J. Fluid Mech. **702**, 415–443 (2012).

[19]S. M. E. Rabin, C. P. Caulfield, and R. R. Kerswell, "Triggering turbulence efficiently in plane couette flow," J. Fluid Mech. **712**, 244–272 (2012).
[20]S. Cherubini, P. de Palma, J.-C. Robinet, and A. Bottaro, "The minimal seed of turbulent transition in the boundary layer," J. Fluid Mech. **689**, 221–253 (2011).
[21]S. Cherubini and P. de Palma, "Nonlinear optimal perturbations in a couette flow: bursting and transition," J. Fluid Mech. **724**, 251–279 (2013).
[22]R. R. Kerswell, C. C. T. Pringle, and A. P. Willis, "An optimisation approach for analysing nonlinear stability with transition to turbulence in fluids as an exemplar," Rep. Prog. Phys. (2014).
[23]B. Hof, A. Juel, and T. Mullin, "Scaling of the turbulence transition in a pipe," Phys. Rev. Lett. **91**, 244502 (2003).
[24]J. Peixinho and T. Mullin, "Finite amplitude thresholds for transition in pipe flow," J. Fluid Mech. **582**, 169–178 (2007).
[25]M. Avila, F. Mellibovsky, N. Roland, and B. Hof, "Streamwise-localised solutions at the onset of turbulence in pipe flow," Phys. Rev. Lett. **110**, 224502 (2013).
[26]M. Chantry, A. P. Willis, and R. R. Kerswell, "Genesis of streamwise-localized solutions from globally periodic travelling waves in pipe flow," Phys. Rev. Lett. **112**, 164501 (2014).
[27]Y. Duguet, A. Monokrousos, L. Brandt, and D. S. Henningson, "Minimal transition thresholds in plane couette flow," Phys. Fluids **25**, 084103 (2013).
[28]F. Mellibovsky and A. Meseguer, "Critical threshold in pipe flow transition," Phil Trans. Roy. Soc. A **367**, 545–560 (2009).
[29]S. M. E. Rabin, C. P. Caulfield, and R. R. Kerswell, "Designing a more nonlinearly stable laminar flow via boundary manipulation," J. Fluid Mech. **738**, R1 (2014).